

Mapping Photolysis Product Radical Reactivities via Soft Ionization Mass Spectrometry in Acrylate, Methacrylate, and Itaconate Systems

Zachary Szablan, Thomas Junkers, Sandy P. S. Koo, Tara M. Lovestead,
Thomas P. Davis, Martina H. Stenzel, and Christopher Barner-Kowollik*

*Centre for Advanced Macromolecular Design, School of Chemical Sciences and Engineering,
The University of New South Wales, Sydney, NSW 2052, Australia*

Received March 14, 2007; Revised Manuscript Received June 8, 2007

ABSTRACT: Electrospray ionization–quadrupole ion trap mass spectrometry (ESI–MS) was utilized to access the polymeric product spectrum generated by the pulsed laser polymerization (PLP) of methyl acrylate (MA) at $-35\text{ }^{\circ}\text{C}$ in the presence of the photoinitiators 2,2-dimethoxy-2-phenylacetophenone (DMPA), benzoin, benzoin ethyl ether (BEE), and bis(2,4,6-trimethylbenzoyl)phenylphosphine oxide (Irgacure 819) to study the reactivity of primary and potential secondary derived radical fragments from photolytically induced fragmentation. Similarly, the polymeric products generated from the PLP of dimethyl itaconate (DMI) at $0\text{ }^{\circ}\text{C}$ using the aforementioned photoinitiators as well as benzil and 2,2'-azobis(isobutyronitrile) (AIBN) were studied using ESI–MS. The PLP products of methyl methacrylate (MMA) initiated with Irgacure 819 at $-25\text{ }^{\circ}\text{C}$ were also examined. Polymerization systems utilizing Irgacure 819 give complex product spectra due to the formation of second generation radical species resulting in several initiator fragments incorporated into a single polymer chain. Termination products, both combination and disproportionation, were identified with high accuracy. The reactivity of the various derived radical fragments toward the monomers employed is summarized for the current and a previous study in tabular form. Energy deposition into the MA/photoinitiator systems is found to have no influence on the product distributions of the MA polymers produced via photoinitiation under the conditions examined. For various photoinitiators employed, products congruent to that of chain transfer to monomer species in the DMI photopolymerizations are observed, conclusively illustrating that chain transfer to monomer is a significant reaction pathway in itaconate free radical polymerizations.

Introduction

Photopolymerizations constitute an important avenue for the preparation of synthetic polymers in both industry and academia.¹ Knowledge of polymer end group functionalities and the potential modulation of these is of high importance in photolytic processes as such moieties are crucial in determining the reactivity and/or stability properties of the final polymer product. For the analysis of photochemically induced polymerization products with high accuracy, mass spectrometry provides a powerful tool to assess the types of polymer end groups. Thus, key information vital to understanding reaction pathways, improving synthetic procedures and consequently the lifetimes of UV-cured polymers can be obtained. The present study focuses on mapping the reactivities of the decomposition products of various photoinitiators (PIs) employed frequently in UV-curing applications, photoimaging and in kinetic studies (see, for example, refs 2–5). Thereby, focus is put on the efficiency of the initiator-derived radical fragments toward initiating and terminating chain growth.

Polymer end group analysis has been revolutionized by the rise of soft-ionization mass spectrometry techniques; namely matrix assisted laser desorption and ionization time-of-flight mass spectrometry (MALDI–ToF–MS)^{6,7} and electrospray ionization–mass spectrometry (ESI–MS) coupled with quadrupole ion trap and/or time-of-flight detectors.^{8–10} The potential of mass spectrometric analysis for synthetic polymers has been discussed in numerous publications and review articles.^{11–14} The accessible mass range for MALDI–ToF–MS is significantly

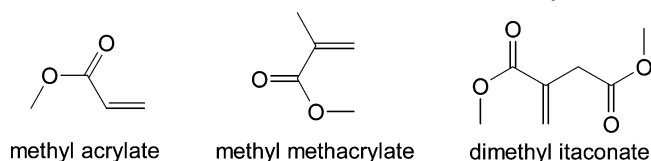
larger ($m/z \sim 100\,000$ amu) than for ESI–MS ($m/z \sim 4000$ amu); however, ESI–MS, due to its very high mass accuracy, allows for unambiguous characterization of intact polymers.¹⁵ ESI coupled with an ion trap provides a molar response to oligomers and fragmentation of oligomers does not occur under various ESI–MS conditions. Therefore, it is possible to obtain repeat unit and end group masses.¹⁵ Both the MALDI and ESI–MS techniques have been employed to study mechanistic aspects of both conventional and living free radical polymerizations (FRP) as well as to conduct fundamental kinetic investigations.^{16–21}

In a recent study, we investigated the radical reactivities of several PI photolysis products toward the tertiary propagating methyl methacrylate (MMA) monomer.²² However, to obtain as complete as possible a picture of the reactivities of various photolysis products from differing PIs in FRP (under a range of reaction conditions) it is mandatory to examine other classes of monomers. Hence, the previous study on MMA²² is extended to the analogous monomers of the acrylate (i.e., methyl acrylate (MA)) and itaconate (i.e., dimethyl itaconate (DMI)) monomer families to cover a broad range of propagating radical reactivities. The propagation rate coefficient (k_p) of MMA at $25\text{ }^{\circ}\text{C}$ is $323\text{ L}\cdot\text{mol}^{-1}\cdot\text{s}^{-1}$ ²³ while MA (at an equivalent monomer concentration) is approximately 50 times faster²⁴ ($k_p = 15\,600\text{ L}\cdot\text{mol}^{-1}\cdot\text{s}^{-1}$). Alternatively, DMI is slower than MMA by a factor of approximately 30 ($k_p = 9.6\text{ L}\cdot\text{mol}^{-1}\cdot\text{s}^{-1}$).²⁵ Scheme 1 depicts the monomers examined in this study.

In addition to the structural likeness between MA and MMA, several further reasons favor the selection of MA for this study. MA has been studied extensively with regard to its mechanistic pathway including propagation,^{24,26} termination²⁷ and chain transfer reactions.^{28,29} Moreover, acrylates are of special interest due to the formation of so-called midchain radicals, generated

* Author to whom correspondence should be addressed. E-mail: camd@unsw.edu.au; c.barner-kowollik@unsw.edu.au. Telephone: +612 9385 4331. Fax: +612 9385 6250.

Scheme 1. Monomers Examined in This Study



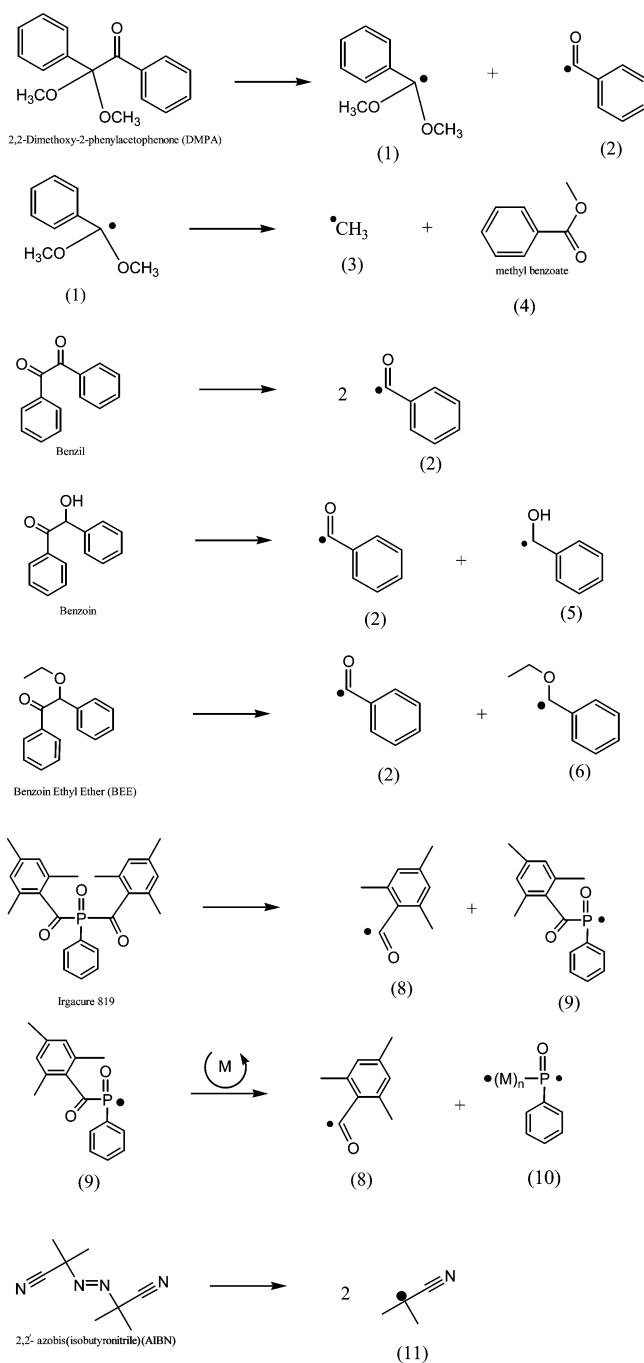
via *intra*- or *intermolecular* chain transfer to polymer reactions via a hydrogen shift. Hereby, the radical center is transferred from the terminal chain unit to a carbon atom on the polymer backbone that is activated by an ester moiety to form a more stable tertiary radical.^{30,31} The formation of midchain radical species has been found to be the cause of unstructured molecular weight distributions obtained with the pulsed laser polymerization–size exclusion chromatography (PLP–SEC) technique,^{32,33} and thus, the inability to gain accurate kinetic data for MA using the PLP–SEC technique under standard conditions above room temperature.³⁴ In-depth characterization of the PI induced polymeric products may significantly contribute to resolving the obstacles arising from these transfer reactions as the loss of characteristic polymer distributions from PLP–SEC can, in principle, not be overcome and hence new routes toward accurate determination of propagation rate coefficients must be taken where mass spectrometry can contribute significantly.

DMI, a sterically hindered monomer was selected judiciously on the basis that it too has been extensively studied with respect to its propagation^{4,25} and termination³⁵ reaction kinetics. DMI (as well as other hindered itaconate species) have been found to display high levels of chain transfer to monomer.^{36,51} A high chain transfer to monomer constant for the itaconate species has been implicated as the marked factor preventing the formation of high molecular weight itaconate polymers with narrow polydispersities using living free radical polymerization techniques as well as the factor responsible for impeding the formation of high molecular weight polymers (i.e., $>10^6$ g·mol⁻¹) from conventional free radical polymerizations of itaconates.^{36,51} Examination of the polymeric product spectrum produced from the photoinitiation of DMI using ESI–MS, even at low temperatures, may show the presence of monomer-initiated species formed as a result of chain transfer to monomer. If present, the observation of monomer-initiated species using ESI–MS would be additional evidence to settle conjecture over the aforementioned hypothesis and would provide valuable information regarding the extent of chain transfer to monomer in these systems.

Corresponding to the previous MMA study²² the photoinitiators 2,2-dimethoxy-2-phenylacetophenone (DMPA), benzoin, benzoin ethyl ether (BEE), benzil, and 2,2'-azobis(isobutyronitrile) (AIBN) are employed (see Scheme 2). These PIs have been studied broadly with respect to their photodecomposition and excited-state products^{37–39} and are common commercial photoinitiators often used in the presence of hydrogen donors. The relative amounts of fragmentation and hydrogen abstraction varies with the type of PI and hydrogen donor as the stability of the free-radicals formed in the photolysis may differ. Since this study is aimed at examining free-radical reactivities of PI photolysis products, and if one considers that hydrogen donors aid in the photo cleavage of the PI clouding the true radical reactivity, no hydrogen donors were employed.

The PIs in this work (except AIBN and Irgacure 819) undergo photochemical α -cleavage from the triplet state by a Norrish Type I mechanism. Benzoin and BEE are used frequently as PIs for vinyl polymerizations due to their fast photochemical

Scheme 2. Photoinitiators Employed and Their Photolysis Radical Products



reaction.¹ Photochemical α -cleavage from the triplet state by a Norrish Type I mechanism yields a benzoyl and an ether type (i.e., alcohol for benzoin) radical and has been shown to be the main process for photolysis of benzoin and its derivatives in a wide temperature range.^{1,40} A major drawback of benzoin ether PIs however is their low thermal stability and associated yellowing of cured coatings.¹ AIBN is an azo-type initiator that undergoes photolysis to yield cyano isopropyl free-radical species and is a major thermal and photoinitiator employed in academic free radical polymerization research studies due to its half-life at mild reaction conditions.⁴¹ Not addressed in our previous study on MMA,²² the photolysis product radical reactivity of Irgacure 819 toward all three monomers (i.e., MA, MMA, and DMI) is examined. Irgacure 819 is a phosphorus centered symmetric compound that may potentially photolytically fragment at two positions to yield a biradical species. The

expected photolysis products of the various photoinitiators are detailed in Scheme 2.

In the current work, ESI–MS analysis is performed on polymers produced by PLP. PLP is used for polymer synthesis because of the molecular weight limitations associated with ESI–MS. PLP can be an efficient and simple technique for obtaining desired molecular weights using photopolymerization and simultaneously allows flexibility in initial initiator and monomer concentrations.⁴² In the PLP technique, the molecular weight of the resulting polymer is controlled by the repetition rate of the incident light radiation under isothermal conditions. The pulsing in PLP induces termination events at the time of the incident light irradiation. Hence, when kinetic parameters are known, desired molecular weights can be targeted.

Coupling the advantages of PLP with the sensitivity of ESI–MS, vital and novel information in regard to the radical reactivities of the various photolysis products produced from common PIs toward MA, MMA, and DMI at low temperatures is obtained for a variety of PI/monomer systems. Fundamental understanding of the photopolymerization mechanism with the overall goal of improving our ability to control photopolymeric material properties is thus enhanced.

Experimental Section

Materials. Methyl acrylate (MA, Aldrich 99%) and dimethyl itaconate (DMI, Aldrich 99%) were deionized by passing over basic alumina. 2,2-Dimethoxy-2-phenylacetophenone (DMPA) (Aldrich 99%), benzil (Aldrich 98%) and benzoin ethyl ether (BEE) (Aldrich 99%) were used as received. Benzoin (Aldrich) and 2,2'-azobis(isobutyronitrile) (AIBN) (DuPont) were recrystallized twice in ethanol prior to use. Irgacure 819 (Ciba 100%) was used as received. Photoinitiator purity was confirmed by ¹H NMR.

Polymerizations. All MA and MMA samples consisted of monomer (sample volume ~ 1.0 mL) with a photoinitiator concentration of 5×10^{-3} mol L⁻¹. DMI samples (sample volume ~ 1.0 mL) had [PI] = 1×10^{-2} mol L⁻¹. Polymerization was achieved by laser pulses generated from a Lambda Physik COMPex Pro 110 XeF (351 nm, 20 ns pulse width) excimer laser system at constant frequencies of 10 to 100 Hz for an overall polymerization time of 20 min for MMA, 50 min for DMI, and 14 s for MA. Single pulse energy ranged between 5 and 25 mJ. More details regarding laser setup and sample methodology have been described previously.²²

Mass Analysis. ESI–MS experiments were carried out using a Thermo Finnigan LCQ Deca ion trap mass spectrometer (Thermo Finnigan, San Jose, CA). The ESI–MS is equipped with an atmospheric pressure ionization source which operates in the nebulizer assisted electrospray mode. The instrument was calibrated with caffeine, MRFA, and Ultramark 1621 (all from Aldrich) in the mass range 195–1822 amu. All spectra were acquired in positive ion mode over the mass to charge range, m/z , 100–2000 Da. The following parameters were used to examine the MA/MMA/DMI systems respectively: spray voltage of 5/5/4.4 kV, a capillary voltage of 39/44/21 V, and capillary temperature of 275 °C in all cases). Nitrogen was used as sheath gas (flow: 40/50/35% of maximum) while helium was used as auxiliary gas (flow: 5% of maximum in all experiments). The eluent was a 6:4 v/v mixture of THF:methanol with an acetic acid concentration of 0.4 mM. Spectra were recorded in positive ion mode with an instrumental resolution of 0.1 amu. All reported molecular weights were calculated via the program package CS ChemDraw 6.0 and are monoisotopic. Simulated isotopic pattern generation was conducted using the Xcalibur program included with the thermo electron ESI–MS. The theoretical molecular weight over charge ratios (m/z , assuming $z = +1$) are calculated using the exact molecular mass of the first isotope within the structure. For the itaconate samples it is important to note that the ESI study was conducted on a monomer/polymer mix due to difficulty in removing the PLP formed polymer from

the monomer sample (DMI monomer is nonvolatile). A monomer/polymer mix was consequently analyzed via ESI, and due to mild suppression of ionization of polymer as a result of the presence of monomer the exceptional quality of the ESI baseline in the following spectra has been somewhat compromised relative to that of the MA and MMA samples as a result of lower signal strength in the ESI–MS.

Size Exclusion Chromatography. Molecular weight distributions (MWD's) for the polymers were measured via SEC on a Shimadzu modular LC system comprising a ERC-3415 solvent degasser, a LC-10AT pump, a SIL-10AD auto-injector, a CTO-10A column oven, and a RID-10A refractive index detector. The system was equipped with a Phenomenex 5.0 μ m bead-size guard column (50 \times 7.5 mm), followed by four Phenomenex columns (10⁶, 10⁴, 10³, 500 Å). The eluent was THF at 40 °C with a flow rate of 1 mL min⁻¹. Calibration curves were generated using polystyrene standards in the molecular weight range 580 to 1.95×10^6 g mol⁻¹. The injection volume was 50 μ L (3–5 mg mL⁻¹). Molecular weights were obtained using the principle of universal calibration employing the Mark–Houwink–Kuhn–Sakurada (MHKS) constants of polystyrene ($K = 14.1 \times 10^{-3}$ mL g⁻¹ and $a = 0.70$),⁴³ polyMA ($K = 19.5 \times 10^{-3}$ mL g⁻¹, $a = 0.660$, THF, 25 °C),⁴⁴ and polyDMI ($K = 46 \times 10^{-3}$ mL g⁻¹, $a = 0.510$, THF, 25 °C).

PolyMA Synthesis Utilizing PLP

As mentioned previously, MA has a much higher propagation rate coefficient than that of both MMA and DMI. Consequently, due to the rate of propagation in conventional MA free radical polymerization, low molecular weight material suitable for ESI–MS analysis is not obtained easily via PLP. The reaction conditions implemented in this study were thus chosen (i.e., low temperatures and high laser pulse frequencies) with the objective of obtaining a “minimum” molecular weight by means of minimizing the chain length. However, as is depicted in Figure 1, even at a temperature of –35 °C and a pulse frequency of 100 Hz, peak molecular weights in the vicinity of 20 000 g·mol⁻¹ are obtained from the PLP of MA irrespective of the PI used.

The first derivative of the MWD depicted in the insert to Figure 1 shows that several points of inflection are observed on the high molecular weight side. The MWD's in Figure 1 fulfill PLP–SEC consistency criteria for k_p determination (BEE shows a significantly less pronounced structuring of the material) with k_p calculated from the inflection points of the MWD in good agreement with literature values.²⁴ However, the pulsing action of the laser only limits chain growth to molecular weights exceeding $10^{5.5}$ g·mol⁻¹. Thus, the polymeric material appears, in the majority, at too high a MW to be examined via ESI–MS. In light of this observation, the MWD's of the PLP products also show large quantities of low molecular weight material which was, with high probability, not terminated by incident laser pulses. PREDICI simulations were undertaken to test for the origin of this low molecular weight polymeric material. These simulations demonstrate that high frequency, high-intensity PLP results in the generation of substantial amounts of short-chain radical species that are not easily observed in conventional calibration GPC analysis (see Figure S1, Supporting Information). The capstone of PLP is that the laser induces termination events that ideally produce a molecular weight distribution with multiple overtones from which the propagation rate coefficient can be deduced (this is indeed observed in the current experiments); however, due to the large population of short chain radicals generated from high-frequency irradiation, conventional termination products (“non-PLP” induced) also occur to some extent. The same simulation of the PLP

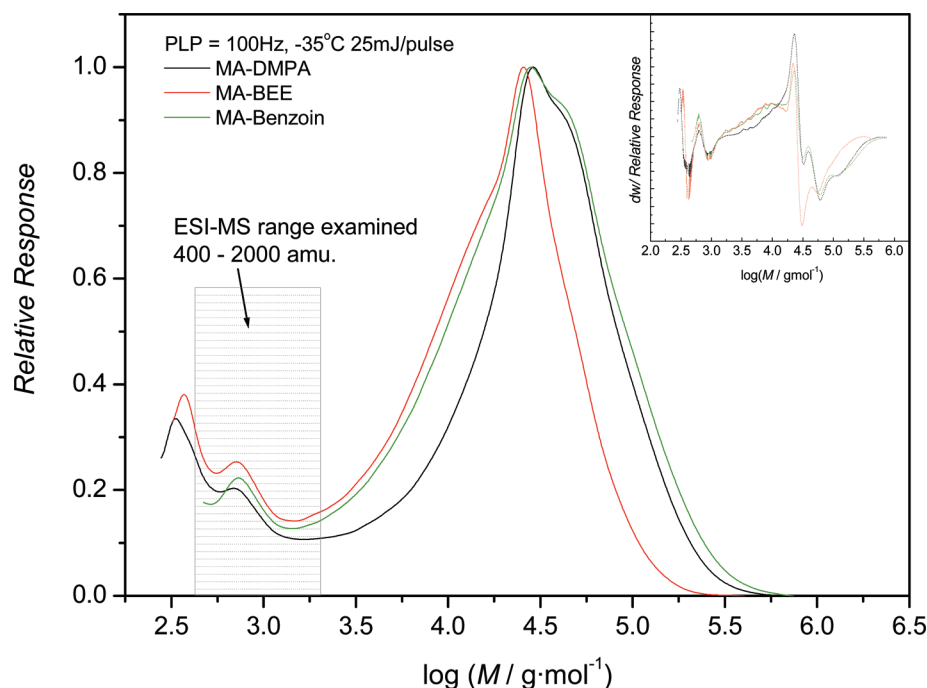


Figure 1. SEC traces of *polyMA* produced via PLP. Reaction conditions and the photoinitiators employed are given within the figure.

experiments (see Figure S1) adequately shows that while the PLP-structured part of the simulated MWD shifts with the laser frequency, low molecular weight material within the accessible ESI–MS mass range is also obtained (see Figure S2). This low molecular weight polymer is formed via combination or disproportionation of (same-sized) growing macroradicals rather than the desired propagating macro free radical species reacting with an initiator photolysis product formed upon laser irradiation to produce dead polymer (the essence of PLP). Nonetheless, polymer product examinable via ESI–MS is formed. It is important to note that photoinitiator derived radical fragments that potentially terminate, rather than initiate chain growth will, in the majority, be built into the higher molecular weight (i.e., PLP portion) of the polymer product. Despite this phenomenon, if present, species containing such products may also be observable—to some extent—in the analysis of the low molecular weight portion of the polymer product.

Nomenclature Definition and Product Identification

Because of the vast amount of polymer products potentially produced in this study, a brief description of the nomenclature used to identify specific products is necessary. All combination products have been labeled $C_{x,y}$ where C represents combination and the subscripts x and y correspond to the numeric values assigned to the photolysis radical fragments (refer to Scheme 2). Similarly, all disproportionation products are labeled $D_{z,1}$ or 2 where subscript z again corresponds to the numeric value assigned to the photolysis radical fragment (the end group fragment) and the subscripts 1 and 2 represent the hydrogen donated and hydrogen abstracted termination products respectively. The * symbol represents an impurity in the baseline of the spectra which is not reproducible between monomer units in the polymer backbone. Unforeseen product peaks are labeled U.

ESI–MS affords the advantage that combination and termination product peaks are in the most part easily distinguished. The isotopic pattern of a combination peak is simple and in the majority of cases can be described as a series of peaks decreasing from left to right on an increasing m/z scale. Dispro-

portionation product peaks are more distinct, that is, they occur in pairs, exactly 2 amu apart. Generally, a set of peaks with maxima 2 amu apart, a smaller peak between them and a series of smaller peaks $1 \times n$ amu's higher in m/z ratio than the primary peak of the product with the greater m/z ratio, are observed. These peaks represent the hydrogen abstracted and hydrogen donated product isotopic patterns respectively. Product spectra may obviously be complicated in a situation where, by chance, multiple product peaks have isotopic patterns that overlap.

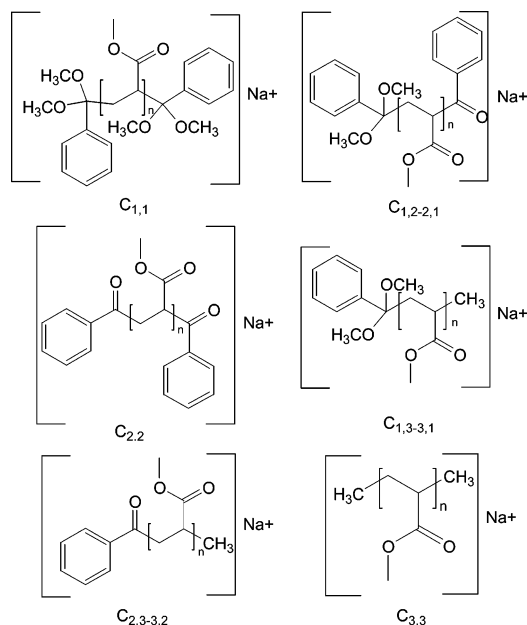
Assignment of ESI-MS Spectra to Product Peaks

Methyl Acrylate. All photopolymerizations of MA were conducted under analogous conditions to enable comparability and provide uniformity to the study as both the temperature and energy deposition dependent behaviors of the radical species produced upon photocleavage must be considered.

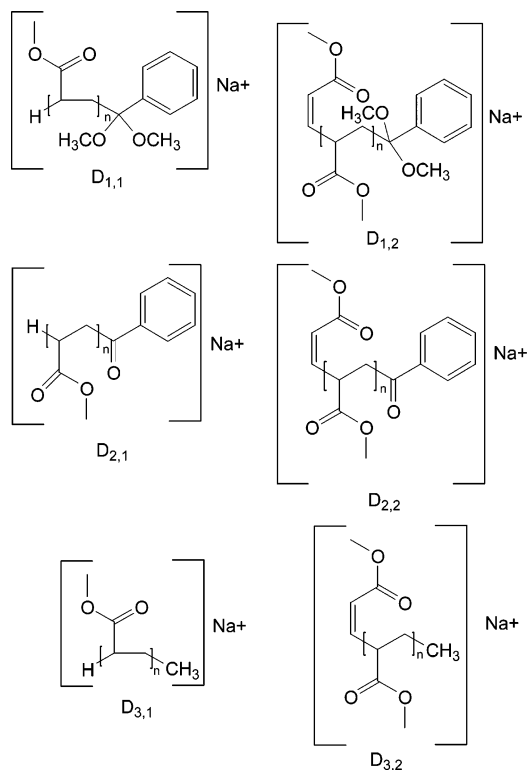
DMPA Initiated PLP of MA. To selectively avoid the formation of byproducts from the photolysis of DMPA¹ and to ascertain the role that the DMPA photolysis products play in initiating and terminating radical chains, low temperatures in conjunction with low irradiation laser intensities were used. In addition, all experiments were conducted in bulk to eliminate any potential chain transfer to solvent reactions. Minimizing reaction temperature serves to restrict the complexity of the resulting polymeric products in that generation of midchain radicals by *inter-* or *intramolecular* chain-transfer to polymer reactions are reduced to a minimum. It has previously been shown that low amounts of midchain radicals are formed under PLP conditions even at -35°C .³⁰ However, as *intramolecular* chain transfer reactions do not change the mass of the radical species, such events will not be mapped by mass spectrometry, nor is it our intention in the current study to do so.

While termination occurs via either combination or disproportionation, the dominant form of termination in MA polymerization is via combination,⁴⁵ albeit that disproportionation also occurs to some extent. Therefore, a variety of polymer products with differing end groups are potentially formed. All probable combination and disproportion termination products in the photopolymerization of MA using DMPA as the PI are presented

Scheme 3. Possible Combination Products Ions Generated via ESI of the Polymeric Material from the Radicals in the DMPA-Initiated PLP of MA



Scheme 4. Possible Disproportionation Product Ions Generated via ESI of the Polymeric Material from the Radicals in the DMPA-Initiated PLP of MA



in Schemes 3 and 4, respectively. The resulting ESI–MS spectra of the PLP produced *poly*MA (for three different laser light intensities) in the mass range 1030 to ~ 1116 m/z are presented in Figure 2.

Major product peaks in the spectra of Figure 2 are assignable to conventional possible products (refer to Table 1). As expected, the product spectra (and all subsequent MA product spectra) provide evidence that MA terminates primarily via combination⁴⁵ with products $\text{C}_{1,1}$, $\text{C}_{1,2-2,1}$, and $\text{C}_{2,2}$ the major product peaks. At this point, it is critical to mention that polymer formed

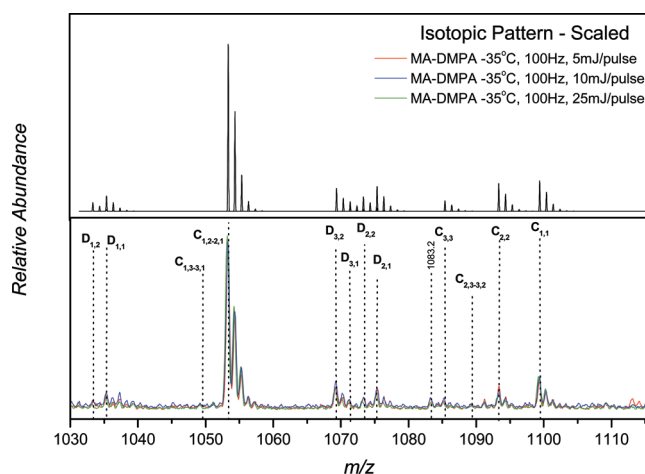


Figure 2. ESI–MS spectra of the polymeric material obtained from the DMPA-initiated ($c_{\text{DMPA},0} = 5 \times 10^{-3}$ mol L^{-1}) PLP of MA_{bulk} at -35°C at various laser intensities and a frequency of 100 Hz (lower part). The simulated isotopic product pattern, scaled to experimental result (100 Hz, 5 mJ/pulse), is given in the upper part of the figure. Theoretical product mass to charge ratios (m/z) are indicated by the dotted lines (see Schemes 3 and 4 for the associated structures).

Table 1. Theoretical and Experimental Molecular Masses of the Combination and Disproportionation Products for the DMPA Initiated PLP of MA_{bulk}

species	m/z_{theor}	molecular formula	m/z_{expt} (5/10/25 mJ)
$\text{C}_{1,1}$	1099.4	$\text{C}_{54}\text{H}_{76}\text{O}_{22}\text{Na}^+$	1099.3
$\text{C}_{1,2-2,1}$	1053.4	$\text{C}_{52}\text{H}_{70}\text{O}_{21}\text{Na}^+$	1053.3
$\text{C}_{2,2}$	1093.4	$\text{C}_{54}\text{H}_{70}\text{O}_{22}\text{Na}^+$	1093.3
$\text{C}_{3,3}$	1085.4	$\text{C}_{50}\text{H}_{78}\text{O}_{24}\text{Na}^+$	
$\text{C}_{2,3-3,2}$	1089.4	$\text{C}_{52}\text{H}_{74}\text{O}_{23}\text{Na}^+$	
$\text{C}_{1,3-3,1}$	1049.4	$\text{C}_{50}\text{H}_{74}\text{O}_{22}\text{Na}^+$	
$\text{D}_{1,1}$	1035.4	$\text{C}_{49}\text{H}_{72}\text{O}_{22}\text{Na}^+$	1035.3
$\text{D}_{1,2}$	1033.4	$\text{C}_{49}\text{H}_{70}\text{O}_{22}\text{Na}^+$	1033.3
$\text{D}_{2,1}$	1075.4	$\text{C}_{51}\text{H}_{72}\text{O}_{23}\text{Na}^+$	1075.4
$\text{D}_{2,2}$	1073.4	$\text{C}_{51}\text{H}_{70}\text{O}_{23}\text{Na}^+$	1073.4
$\text{D}_{3,1}$	1071.4	$\text{C}_{49}\text{H}_{76}\text{O}_{24}\text{Na}^+$	
$\text{D}_{3,2}$	1069.4	$\text{C}_{49}\text{H}_{74}\text{O}_{24}\text{Na}^+$	

via combination of a propagating macroradical with a primary initiator-derived radical is not distinguishable from a polymer formed by the head-to-head coupling of two growing polymer chains initiated via the same initiator fragments. Therefore, as no direct quantitative calculations are made and the key focus lies in photolysis product reactivity, it is inconsequential to the principle of this study as to whether the analyzed polymer was formed by the pulsing action of the laser or via “conventional” termination in the dark time between two pulses.

The use of various reaction conditions, photoinitiators, and monomers in this study makes the discussion of individual reactions both tedious and longwinded. We therefore limit the discussion section for each monomer/PI system to detail only the major implications of the various systems. To summarize, a thorough comparison of the photolysis fragment reactivity toward the various monomers is provided in the final section of this contribution.

Figure 2 shows evidence that products congruent to both those of disproportionation and combination incorporating both the acetal and benzoyl fragments are found, leading to the conclusion that both the benzoyl and acetal fragments generated as a result of DMPA photocleavage seem to initiate and highly likely terminate MA polymerization. The relative amounts of each product are an indicator of the likelihood of radicals to terminate or initiate the growing polymer chain. Looking first at the combination products, product $\text{C}_{1,1}$ is more abundant than product $\text{C}_{2,2}$, which may suggest that the acetal fragment is a

more effective terminating species under these conditions than that of the benzoyl radical (assuming that both the fragments have an equal propensity to initiate the polymerization). Conversely, the acetal radical may be more likely to initiate polymerization. This finding is in agreement with fragment **1** being more likely to terminate the chain reaction as was previously observed in a similar DMPA/MMA system²² and gives clarity to the fact that $C_{1,2-2,1}$ is the dominant species.

As disproportionation products contain the initiating photolysis fragment only, they provide further information on the photolysis products predisposition to initiate or terminate polymerization. The quantitative abundance of products $D_{1,1}$, $D_{1,2}$, $D_{2,1}$, and $D_{2,2}$ suggest, (safely assuming that the initiated species have equal propensity to terminate via disproportionation), that the benzoyl radical is slightly more reactive than the acetal radical as the abundance of disproportionation products $D_{2,1}$ and $D_{2,2}$ is somewhat greater than that of $D_{1,1}$ and $D_{1,2}$. Product peaks at $m/z = 1069.4$ and 1071.4 are observed and may potentially be assigned to structures $D_{3,2}$ and $D_{3,1}$ respectively; hence implying that a secondary fragmentation of the acetal (**1**) radical is occurring¹ and that the methyl radicals produced effectively initiate polymerization. However, the characteristic shape of the isotopic pattern with a maximum at $m/z = 1069.4$ suggest that this product peak is an unexpected combination product rather than a disproportionation product. Such an observation keeps steady with the hypothesis that the methyl radical acts almost exclusively as a terminating species.²² Minute amounts of polymer product congruent with $m/z = C_{3,3}$ are found. However, the product peak at $m/z = 1085.2$ appears to be part of an unexpected disproportionation product due the characteristic shape of this distribution with the presence of a polymer product peak at $m/z = 1083.2$. In either case, this finding suggests that, if present, the methyl radical is unlikely to initiate polymerization. No polymer products congruent with products ($C_{1,3-3,1}$ or $C_{2,3-3,2}$) are identified in the product spectra. Therefore, it is tentatively concluded that secondary fragmentation of the acetal radical, although potentially occurring, does not significantly affect the type of polymer products produced (in the MW range examined). This hypothesis is strengthened further by the fact that energy input into the polymerizable reaction mixture did not influence the types of polymer products formed. Laser light intensity, in principle, has a pronounced effect on the photolysis products of DMPA.¹ To this end, the radiation laser intensity was increased step wise from 5 to 25 mJ/pulse and under the conditions examined it was shown that the total amount of primary radicals generated on firing a laser pulse does not influence the resulting product spectrum, at least in the MW range investigated.

Benzoin-Initiated PLP of MA. The resulting mass spectra obtained are shown in Figure 3. Again, no influence from increased energy deposition into the system was observed. Possible combination and disproportionation termination products incorporating the alcohol fragment from the benzoin-initiated PLP of MA are depicted in Schemes S1 and S2 with theoretical and experimental m/z values of possible product ions listed in Table S2.

Both the benzoyl and alcohol fragments generated as a result of benzoin photocleavage are interpreted to initiate and highly likely terminate polymerization. This statement is clarified upon examination of the product spectra. In analyzing the combination product peaks, peak $C_{5,2-2,5}$ is the largest, suggesting that either species **2** or **5** is a dominant terminating species or that both species initiate polymerization. Product peak $C_{2,2}$ is clearly present suggesting that the benzoyl fragment is effective in

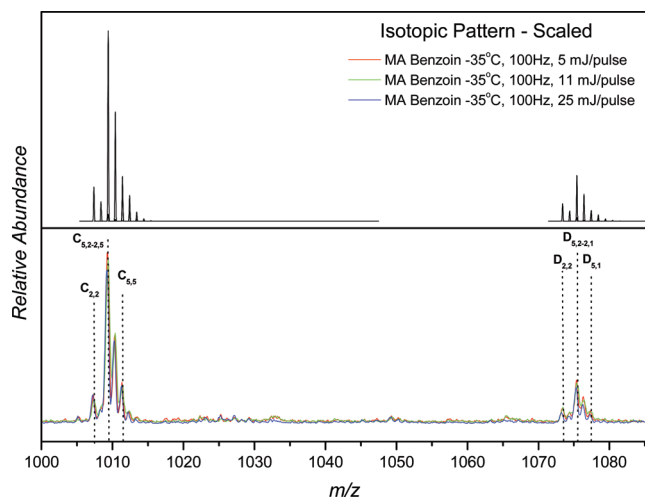


Figure 3. ESI-MS spectra of the polymeric material obtained from the benzoin-initiated ($C_{\text{benzoin},0} = 5 \times 10^{-3} \text{ mol L}^{-1}$) PLP of MA_{bulk} at -35°C at various laser intensities and a frequency of 100 Hz (lower part). The simulated isotopic product pattern, scaled to experimental result (100 Hz, 5 mJ/pulse), is given in the upper part of the figure. Theoretical product mass to charge ratios (m/z) are indicated by the dotted lines (see Schemes S1 and S2 for the associated structures). Reaction conditions are given within the figure.

initiating polymerization, with quantitative amounts of products $D_{5,2-2,1}$ and $D_{2,2}$ endorsing this notion. When examining the alcohol fragment reactivity, the quantitative abundance of products $C_{5,5}$ and $D_{5,2}$ is not so clear-cut and making a direct conclusion is difficult. Remembering that disproportionation is the minor termination pathway in the system, the potential presence of small quantitative amounts of product $D_{5,1}$ and $C_{5,5}$ would indicate that the alcohol radical initiates polymerization to some extent. The data presented, however, do not allow for the conclusion that the alcohol fragment is unable to initiate under these conditions and hence we attribute its reactivity as being primarily terminating.

BEE-Initiated PLP of MA. BEE was employed to determine whether a change in the structure of the “ether type” fragment significantly affects the PI reactivity (compared to that of DMPA and benzoin). The theoretical and experimental m/z values of the combination and disproportionation product ions of the BEE-initiated PLP of MA are given in Table S3 and the chemical structures of the termination products incorporating the ether type radical are depicted in Schemes S3 and S4 respectively.

Products $C_{6,2-2,6}$ and $C_{2,2}$ are, as expected, the dominant product species (refer to Figure 4). The presence of quantitative amounts of disproportionation products $D_{2,1}$ and $D_{2,2}$ advocates that the benzoyl fragment initiates polymer chain growth. The ability of the ether fragment to initiate polymerization is questionable. The near total absence of product peak $C_{6,6}$ as well as $D_{6,1}$ and $D_{6,2}$ support the hypothesis that the ether fragment acts almost exclusively as a terminating moiety, especially when taking into account that the ether and benzoyl fragments have an affinity to form $C_{6,2-2,6}$: $C_{6,6}$: $C_{2,2}$ in the ratio of (2:1:1) (assuming that they equally initiate chain-growth) and that $C_{2,2}$ largely dominates product $C_{6,6}$. However, a product peak that is highly likely a combination peak at $m/z = 1019.2$, congruent to disproportionation product $D_{6,1}$, casts some doubt on this hypothesis. On the other hand, absence of disproportionation product $D_{6,2}$ (which should theoretically be present in close to equal quantities to $D_{6,1}$) coupled with almost negligible quantities of $C_{6,6}$ suggest that the peak found at $m/z = 1019.2$ is more likely due to some other species whose origin, at present, remains unknown.

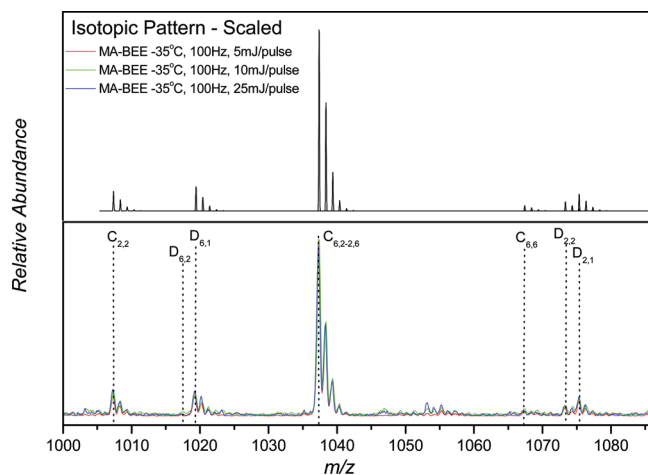


Figure 4. ESI-MS spectra of the polymeric material obtained from the benzoin ethyl ether initiated ($c_{\text{BEE},0} = 5 \times 10^{-3} \text{ mol L}^{-1}$) PLP of MA at -35°C , at a frequency of 100 Hz (lower part). The simulated isotopic product pattern, scaled to experimental result (100 Hz, 5 mJ/pulse), is given in the upper part of the figure. Theoretical product mass to charge ratios (m/z) are indicated by the dotted lines (see Schemes S3 and S4 for the associated structures). Reaction conditions are given within the figure.

Irgacure 819 Initiated PLP of MA. The photolysis products of bis(2,4,6-trimethylbenzoyl)phenylphosphine oxide (Irgacure 819) are of specific interest for several reasons. First, Irgacure 819 is a widely used commercially available PI.⁴⁶ More interestingly, this PI may fragment to yield a phosphorus centered biradical species which may initiate polymerization. While it is unlikely that a biradical will form during photodissociation of the Irgacure PI, bond cleavage to either side of the phosphorus atom may occur throughout the reaction. As product analysis does not allow for kinetic information to be drawn from it, the core $\text{P}=\text{O}$ fragment can, for simplicity, be treated as a biradical. Furthermore, acylphosphine oxides have been shown

to be highly reactive toward acrylates⁴⁷ with the high reactivity ascribed to the phosphinyl radicals generated.⁴⁸

Complementary interest in Irgacure 819 arises from the additional methyl moieties on the benzoyl fragment produced upon photolysis. These moieties may significantly influence the photolysis products stability resulting in a reactivity differing from that of the nonsubstituted benzoyl fragment produced in the photolysis of, e.g., DMPA and benzoin. Possible combination and disproportionation products generated as a result of the photopolymerization of MA in the presence of Irgacure 819 are given in Schemes S5 and S6, respectively. Because of the potential biradical nature of the PI, as well as combination and disproportionation products specifically, hybrid disproportionation/combination products and products involving multiple $\text{P}=\text{O}$ fragments are also possible (see Scheme S7). The resulting complex product spectrum for an Irgacure 819 initiated MA sample is given in Figure 5.

Quantitative amounts of disproportionation (i.e., $\text{D}_{9,1}$ and $\text{D}_{9,2}$) and hybrid combination/disproportionation products (e.g., $\text{D}_{10,1}\text{C}_9$ and $\text{D}_{10,2}\text{C}_9$) are formed (refer to Table S4 for the theoretical and experimental m/z values of the combination and disproportionation as well as hybrid product ions of the MA/Irgacure 819 system). The presence of disproportionation products $\text{D}_{8,1}$ and $\text{D}_{8,2}$ as well as $\text{D}_{9,1}$ and $\text{D}_{9,2}$ indicate that both the initial photolysis product fragments of Irgacure 819 (i.e., **8** and **9** refer to Scheme 2) initiate polymerization. The presence of products congruent with hybrid combination/disproportionation products illustrate that the phosphorus radical (**9**) can undergo secondary fragmentation to form radicals **10** and **8** in a 1:1 ratio (refer to Scheme 2). On the basis of the quantitative proportions of products $\text{D}_{8,n}$ and $\text{D}_{9,n}$, it may be assumed (when all initiated species have an equal propensity to terminate via disproportionation) that photolysis fragment **9** is more reactive than **8** as a greater amount of polymer corresponding to $\text{D}_{9,n}$ than $\text{D}_{8,n}$ is formed. Such a finding is further supported by the notion that the quantity of **8** should be greater than **9** due to the secondary

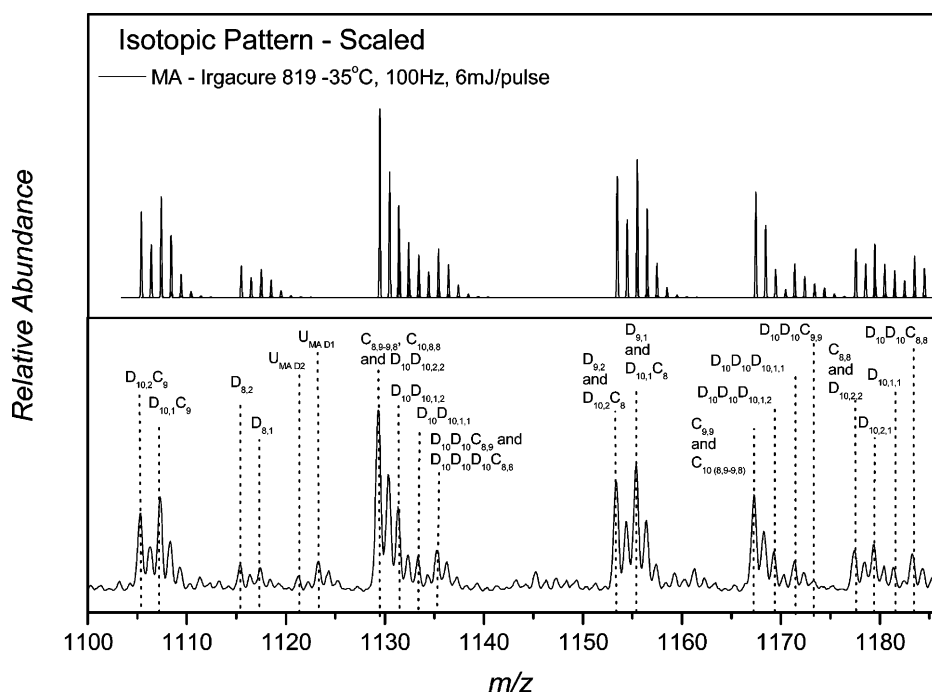


Figure 5. ESI-MS spectrum of polymeric material obtained from the Irgacure 819 initiated ($c_{\text{Irg819},0} = 5 \times 10^{-3} \text{ mol L}^{-1}$) PLP of MA_{bulk} (lower part). The reaction conditions are given within the figure. The theoretical isotopic pattern distribution, scaled to the experimental result is given in the upper part of the figure. Theoretical product mass to charge ratios are indicated by the dotted lines.

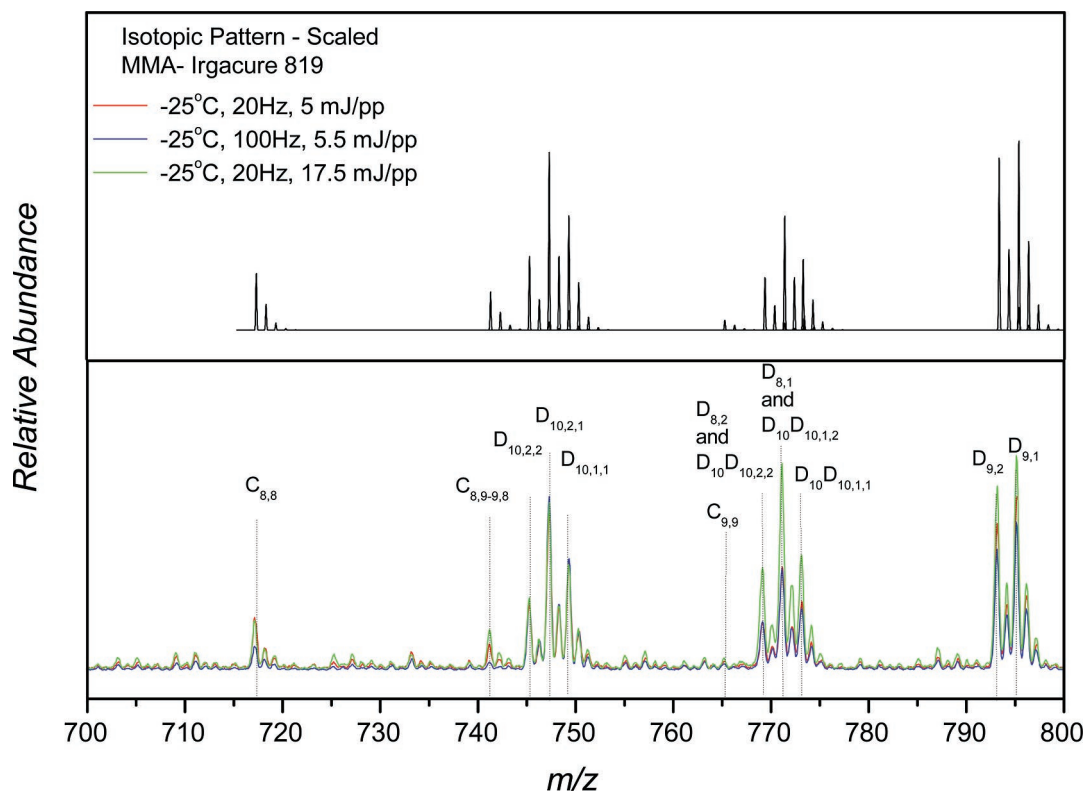


Figure 6. ESI-MS spectra of polymeric material obtained from Irgacure 819 initiated ($c_{\text{Irg819},0} = 5 \times 10^{-3} \text{ mol L}^{-1}$) PLP of MMA_{bulk} (lower part). The reaction conditions are given within the figure. The theoretical isotopic pattern distribution, scaled to the experimental result (-25°C , 20 Hz, 5 mJ/pulse), is given in the upper part of the figure. The results are normalized at $m/z = 747.3$, and theoretical product mass to charge ratios are indicated by the dotted lines.

fragmentation of **9** and aligns with findings by Baxter and Davidson⁴⁸ in a study of the photodecomposition of diphenyl-2,4,6-trimethylbenzoyl-phosphine oxide in the presence of 1,1-di-*p*-tolylethylene.

When considering the presence of hybrid combination/disproportionation products or disproportionation products containing multiple fragment **10**'s in the polymer backbone, the presence of species $\text{D}_{9,n}$ and $\text{C}_{9,9}$ indicate that large quantities of polymer product is generated which at a later stage may potentially undergo photodissociation in the presence of varying monomer species to generate block copolymers of almost any composition without the use of living/controlled polymerization techniques. In effect, combination or disproportionation products involving fragment **9** can be viewed as macroinitiating species.

The assignment of the MA/Irgacure 819 spectrum is complicated by a diverse amount of product formation. Dissociation of any compound incorporating fragment **9** yields a "new generation" of polymers which again have the opportunity to terminate via combination with other (macro)molecules, photolysis products or via disproportionation. While the ability to view each new generation of polymer species with increasing degree of polymerization is reduced in the assignment in Figure 5 by the limited mass range examined, a large number of possible polymer products, often congruent in m/z ratio, and therefore indistinguishable, are still formed. Evidently, therefore, as the degree of polymerization in the system increases so too does the complexity and range of the polymer species produced.

The complexity of the spectra in Figure 5 is further enhanced by the formation of puzzling product species (denoted $\text{U}_{\text{MA D},n}$). The m/z values of the peak maxima of these products are listed in Table S4. These products are not congruent with any MA polymer products shown in the structure lists in the Supporting

Information. Furthermore, the S/N ratio in Figure 5, for reasons previously discussed, make it difficult to ascertain if greater amounts of unexpected polymer products are definitely present. In spite of this, assignable product peaks dominate the spectrum with unexpected product peaks, collectively, constituting less than approximately 3% of the total polymer product.

Methyl Methacrylate. Irgacure 819 Initiated PLP of MMA. To aid in assigning the complex Irgacure 819/MA spectra, an analogous experiment was carried out for MMA. Possible combination, disproportionation and hybrid combination/disproportionation products for the Irgacure 819/MMA system are depicted in Schemes S8, S9, and S10. Figure 6 shows the resulting product spectra obtained for different laser light intensities. Spectra of high resolution are obtained (refer to Table S5). Interestingly, increasing the frequency of irradiation or intensity of irradiation does not result in the formation of unexpected polymer products, unlike what was observed in DMPA-, benzoin-, and BEE-initiated MMA systems.²² This finding supports further the notion that the unexpected polymer products found in our previous MMA study²² result from the non-benzoyl photolysis product fragment formed in Type I photoinitiator cleavage as Irgacure 819 also yields benzoyl-type radicals. Furthermore, Figure 6 illustrates that, as expected, disproportionation is the dominant mode of termination in the MMA/Irgacure 819 system²² with products $\text{D}_{10,1,1}$, $\text{D}_{10,2,1}$, and $\text{D}_{10,2,2}$ (refer to Scheme S10) prominent in the low intensity and frequency experiments. These products are congruent with polymer structures incorporating a phosphorus centered molecule **10** (derived from the secondary photolysis of photolysis product **9**), which are disproportionation products.

In comparing the Irgacure 819 MMA and MA data, a high proportion of material consisting of products that can be assigned to contain fragment **10** are identified in both cases, thus leading

to the conclusion that further photodissociation of **9** is not monomer dependent. Both systems evidence that disproportionation products $D_{9,1}$ and $D_{9,2}$ are more predominant than those of $D_{8,1}$ and $D_{8,2}$ further supporting results by Baxter and Davidson⁴⁸ that the phosphinyl radical is the dominant initiating species in acrylate systems when phosphine oxide initiators are used.

The presence of disproportionation products $D_{8,1}$ and $D_{8,2}$ as well as $D_{9,1}$ and $D_{9,2}$ (also $D_{10,1}C_8$ and $D_{10,2}C_8$, respectively) indicate that both fragments **8** and **9** in Scheme 2 initiate polymerization. The presence of significant amounts of products $C_{8,8}$ as well as $C_{8,9-9,8}$ (also $C_{10,8,8}$) along with the absence of combination product $C_{9,9}$ infer that photolysis product **8** is less effective as an initiating species than the phosphorus radical **9**. However, the quantitative differences may result from the secondary fragmentation of photolysis product **9**, allowing $C_{9,9}$ to act as a macrophotoinitiating species that may undergo fragmentation at each/either of the chain ends to yield adduct **8**, forming hybrid combination/disproportionation products incorporating fragment **9** thus result in the formation of a “new generation” of products (refer to Scheme S10). Through further photolysis, polymer products incorporating 2 or more of fragment **10** in the polymer backbone can be produced. The presence of quantitative amounts of product $D_{10}D_{10,1,1}$, $D_{10}D_{10,1,2}$, and $D_{10}D_{10,2,2}$ ($m/z = 773.2$, 771.2 , and 769.3 respectively) is direct proof of this. Therefore, it is no surprise that increased laser intensity (17.5 mJ/pulse, 20 Hz) increases quantitative proportions of these products, in all probability a result of a greater proportion of secondary fragmentation. However, the MMA data allow for a better quantitative understanding of the product distributions as the spectra are less complex due to the high propensity of MMA to terminate almost exclusively via disproportionation. A situation in which 3 or more of fragment **10** are incorporated in the polymer backbone is not possible in the MW range given in Figure 6.

Dimethyl Itaconate. Analogous conditions were used for all the DMI/PI systems examined and product spectra evidence that DMI terminates primarily via disproportionation as previously reported.³⁵

DMPA-Initiated PLP of DMI. Polymer samples were produced via PLP at a reaction temperature of 0 °C and reaction frequencies of 10 to 20 Hz. Figure 7 exhibits the resulting spectra. Theoretical combination and disproportionation products are given in Schemes S11 and S12 respectively with the corresponding m/z values of the product ions listed in Table S6.

The presence of product peaks congruent with disproportionation products $D_{1,n}$ and $D_{2,n}$ implies that both the benzoyl and acetal fragments generated as a result of DMPA photocleavage initiate and highly likely terminate DMI polymerization. Interestingly, it is found that the disproportionation product peaks $D_{1,n}$ are quantitatively greater than that of $D_{2,n}$ suggesting that the acetal radical is the superior initiating species (again, assuming that both types of initiated species have equal propensity to terminate via disproportionation). This observation is somewhat surprising and may arise as a consequence of DMI's hindered nature, restricting the ability of the photolysis product to access the vinyl site of the monomer to initiate propagation, or, more likely, DMI's slow propagation and termination rate renders the reactivity of the photolysis fragments (i.e., **1** and **2**) less biased, therefore allowing the acetal radical to become more involved in the reaction. It is also possible that the elevated temperature of the system, (i.e., 0 °C) as compared

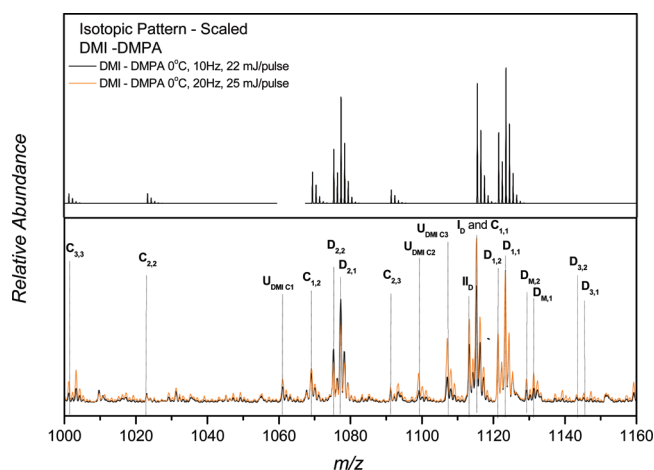


Figure 7. ESI-MS spectra of polymeric material obtained from DMPA-initiated ($C_{DMPA,0} = 1 \times 10^{-2}$ mol L⁻¹) PLP of DMI_{bulk} (lower part). The reaction conditions are given within the figure. The theoretical isotopic pattern distribution, scaled to the experimental result (0 °C, 10 Hz, 22 mJ/pulse), is given in the upper part of the figure. The results are normalized at $m/z = 1123.5$, and the theoretical product mass to charge ratios are indicated by the dotted lines.

to that of the MMA and MA systems, leads to the various fragments having a different reactivity.

Additionally, product peak $C_{2,2}$ is nearly absent, which may be attributed to the dominance of both termination via disproportionation and the acetal radical's ability to act as an initiating species toward DMI. A large peak congruent to $C_{1,1}$ may further suggest that the acetal fragment is the dominant initiating species in the system. However, $C_{1,1}$ is congruent to DMI- I_D . This peak at $m/z = 1115.4$ (in conjunction with DMI- II_D ; see Scheme S13 for structures) is expected to occur analogous to the results previously reported for DMPA-initiated MMA as well as DMPA-initiated *n*-butyl methacrylate (BMA) polymerizations.²² DMI- I_D and - II_D are polymers that are disproportionation products which occur in large quantitative amounts relative to the theoretically expected product peaks. Unfortunately, a mechanism to explain these unexpected product species is lacking, and regardless of the origin of the disproportionation peak, no quantification of species $C_{1,1}$, is possible.

Figure 7 reveals quantitative amounts of disproportionation products at $m/z = 1131.4$ and 1129.4 (labeled $D_{M,1}$ and $D_{M,2}$ respectively). These products are congruent with monomer-initiated polymer chains terminated via disproportionation (refer to Scheme S13) providing evidence that chain transfer to monomer occurs under the experimental conditions investigated here. Numerous studies have indicated that itaconate monomers undergo chain transfer to monomer reactions due to the presence of labile hydrogen atoms next to the vinyl bond.^{49,50} The presence of quantitative amounts of chain transfer to monomer products, even at low conversion, provides further evidence to support claims that transfer to monomer is the cause of broadening in the molecular weight distributions with increasing conversion in reversible addition fragmentation chain transfer (RAFT) mediated living free radical polymerizations of DMI observed at 60 °C.⁵¹ The chain transfer to monomer constant (C_m) for DMI at 60 °C has been shown to be 1.4×10^{-3} .⁵¹ Considering that C_m is not overly temperature dependent, it is no great surprise that chain transfer to monomer products are observed at 0 °C. However, the chain transfer to monomer reaction may be reduced significantly for the lower chain-length itaconate propagating species.

Moreover, Figure 7 shows the presence of 3 unexpected combination products (i.e., $U_{DMI\ C1,C2}$ and C_3) (refer to Table S6)

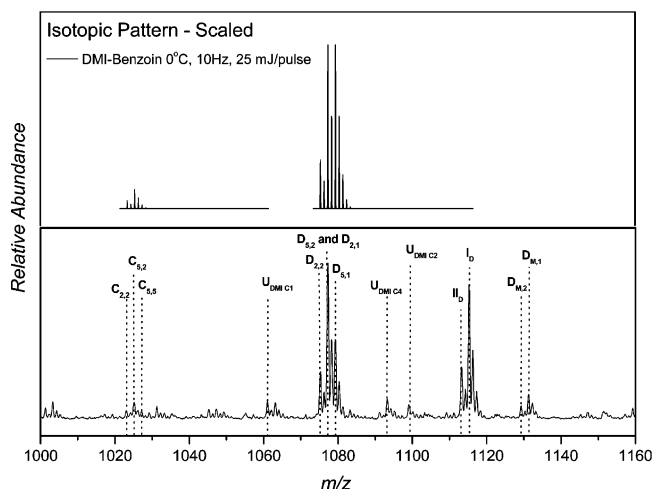


Figure 8. ESI-MS spectrum of polymeric material obtained from the benzoin-initiated ($c_{\text{benzoin},0} = 1 \times 10^{-2} \text{ mol L}^{-1}$) PLP of DMI_{bulk} (lower part). The reaction conditions are given within the figure. The theoretical isotopic pattern distribution scaled to the experimental result is given in the upper part of the figure. Theoretical product mass to charge ratios are indicated by the dotted lines.

that are *not* congruent with any typical polymeric species obtainable from “conventional” photolysis of DMPA and reaction with DMI. The absence of any significant quantitative amounts of disproportionation products $\text{D}_{3,1}$ and $\text{D}_{3,2}$, coupled with the presence of almost negligible quantities of product congruent with combination product $\text{C}_{2,3-3,2}$ lead to the tentative conclusion that the methyl radical produced as a result of secondary fragmentation of the acetal radical acts almost exclusively as a terminating species. The presence of polymer product congruent to combination product $\text{C}_{3,3}$ is also found at $m/z = 1001.4$; however, this peak appears to be part of an unidentified disproportionation peak (based on its characteristic isotopic distribution) and thus, this product peak is not assigned with confidence. Interestingly, the peak identified as $\text{C}_{3,3}$ in the DMPA-initiated MA polymerization also shows an isotopic pattern otherwise typical of disproportionation, strengthening the hypothesis that (almost) no $\text{C}_{3,3}$ is formed in either polymerization.

Benzoin-Initiated PLP of DMI. To ascertain whether or not the complex product spectra observed in the DMPA/DMI systems are a consequence of the hindered nature of the monomer or the initiator, DMI was photopolymerized in the presence of benzoin. Figure 8 presents the resulting mass spectrum. The polymeric structures corresponding to combination and disproportionation termination products are given in Schemes S14 and S15 with theoretical and experimental m/z values listed in Table S7.

The presence of peaks congruent with both product peaks $\text{D}_{2,n}$ and $\text{D}_{5,n}$ suggest that both the alcohol and benzoyl photolysis fragments initiate and highly likely terminate polymerization. This hypothesis is supported by the presence of a small quantitative amount of product peak $\text{C}_{2,5-5,2}$. The near absence of product peaks corresponding to products $\text{C}_{5,5}$ and $\text{C}_{2,2}$ may potentially be attributed to the dominance of disproportionation as the mechanism of termination in the free radical polymerization of DMI under these conditions. Interestingly, as observed in the DMI/DMPA system, large quantitative amounts of products DMI-I_D and DMI-II_D are found. Furthermore, quantitative amounts of $\text{U}_{\text{DMI C1,C2}}$ and C_4 , the formation of which are atypical are observed. Coincidentally, product peaks $\text{U}_{\text{DMI C1}}$ and C_2 appear in relatively the same quantitative amounts in both the DMPA and benzoin DMI spectra, suggesting that

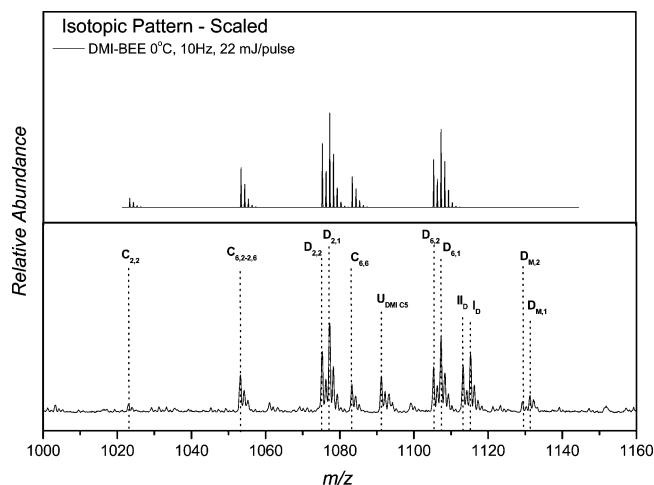


Figure 9. ESI-MS spectrum of polymeric material obtained from the BEE-initiated ($c_{\text{BEE},0} = 1 \times 10^{-2} \text{ mol L}^{-1}$) PLP of DMI_{bulk} (lower part). The reaction conditions are given within the figure. The theoretical isotopic pattern distribution scaled to the experimental result is given in the upper part of the figure. Theoretical product mass to charge ratios are indicated by the dotted lines.

these products arise from reactions related to the benzoyl fragment and/or monomer. Additionally, the presence of quantitative amounts of disproportionation products $\text{D}_{\text{M},1}$ and $\text{D}_{\text{M},2}$ again indicates the incidence of chain transfer to monomer in DMI free radical polymerization.

BEE-Initiated PLP of DMI. Figure 9 presents the resulting mass spectrum with theoretical combination and disproportionation products incorporating the ether type radical given in Schemes S16 and S17 respectively. Corresponding m/z values are listed in Table S8.

The presence of quantitative amounts of products $\text{D}_{2,n}$ and $\text{D}_{6,n}$ indicate that both the ether and benzoyl fragments produced from BEE photolysis are effective in initiating polymerization. Quantitative amounts of products $\text{C}_{6,6}$ and $\text{C}_{6,2-2,6}$ in conjunction with the near absence of product $\text{C}_{2,2}$ suggests that the ether radical is the more prominent terminating species.

Benzil-Initiated PLP of DMI. In a further attempt to determine whether the previously observed trend of product spectrum complexity is related to the non-benzoyl fragment of the PIs examined, DMI was photopolymerized using benzil, where the only photolysis product fragments are that of benzoyl radicals. The resulting mass spectrum is shown in Figure 10. Theoretical and experimental m/z values of the product ions are given in Table S9. Corresponding combination and disproportionation products can be drawn from Schemes S1 and S2, respectively.

Quantitative amounts of chain transfer to monomer disproportionation products $\text{D}_{\text{M},1}$ and $\text{D}_{\text{M},2}$, are observed. A key observation to be noted from Figure 10 is the near absence of disproportionation products I_D and II_D . In the majority, therefore, the formation of these products must be attributed to the non-benzoyl fragment in the presence of DMI monomer for the DMPA, benzoin and BEE-initiated DMI systems. The very same conclusion was drawn from MMA studies utilizing the same PIs.²²

AIBN-Initiated PLP of DMI. To deduce if the cause of the previously observed complex DMI product spectra are related to the DMI monomer for the type I PIs examined, DMI was photopolymerized using azo-initiator 2,2'-azobis(isobutyronitrile) to employ radicals of a completely different type. The resulting mass spectrum is presented in Figure 11.

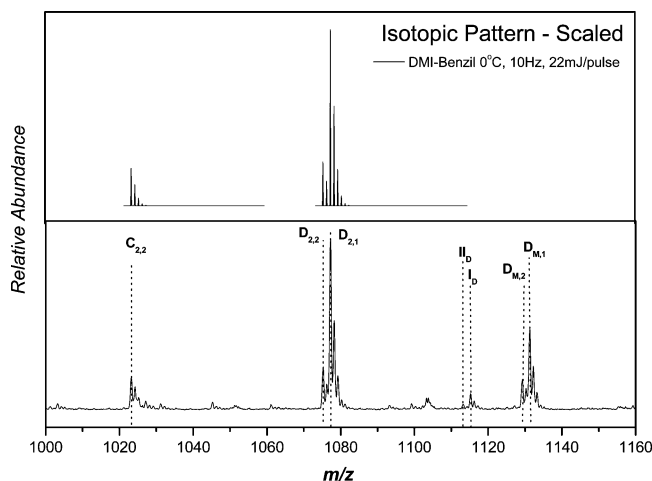


Figure 10. ESI-MS spectrum of polymeric material obtained from the benzil-initiated ($c_{\text{benzil},0} = 1 \times 10^{-2} \text{ mol L}^{-1}$) PLP of DMI_{bulk} (lower part). The reaction conditions are given within the figure. The theoretical isotopic pattern distribution scaled to the experimental result is given in the upper part of the figure. Theoretical product mass to charge ratios are indicated by the dotted lines.

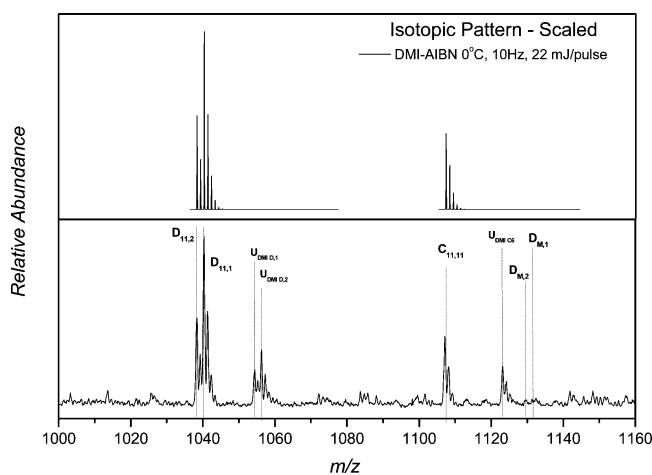


Figure 11. ESI-MS spectrum of polymeric material obtained from the AIBN-initiated ($c_{\text{AIBN},0} = 1 \times 10^{-2} \text{ mol L}^{-1}$) PLP of DMI_{bulk} (lower part). The reaction conditions are given within the figure. The theoretical isotopic pattern distribution scaled to the experimental result is given in the upper part of the figure. Theoretical product mass to charge ratios are indicated by the dotted lines.

Polymeric structures corresponding to termination products for the AIBN-initiated PLP of DMI are given in Scheme S18. Corresponding m/z values of the product ions are listed in Table S10. With the exception of the anticipated disproportionation and combination product ions incorporating the cyanoisopropyl species, unexpected products were observed in substantial quantities. First, quantitative amounts of what are definitely disproportionation products at $m/z = 1056.3$ and 1054.4 are observed. *Prima facie*, the origin of such disproportionation products is as puzzling as the origin of combination products observed in the other DMI systems examined. To complicate matters further, a combination product peak at $m/z = 1122.9$, which was not previously observed in the other DMI systems, is also observed. The origin of the unexpected combination and disproportionation products observed in the mass spectra obtained for the DMI systems is therefore questionable and one may only report that the spectra obtained from the photopolymerization of DMI using various PI's are more complex than anticipated, potentially suggesting a complex mechanism of product formation under the conditions examined. However, as

the itaconate monomers propagate more slowly than almost any other monomer class,⁴ it may be safely assumed that the rate of the first addition of a primary photoinitiator derived radical to a monomer unit is significantly reduced. In consequence, the primary radicals persist for a longer time, in which secondary decomposition reactions may take place (that are, while on a completely different time scale, not too different in nature to the solvent-cage reactions observed for peroxide initiation).⁵²

Irgacure 819 Initiated PLP of DMI. To bring the study of Irgacure 819 full circle, DMI was polymerized in the presence of Irgacure 819. Examination of Irgacure 819 photolysis product reactivity toward DMI may shed light on unexpected product formation in the other PI/DMI systems. The resulting product spectrum is presented in Figure 12. For structures and details on peak assignment see Schemes S19 to S21 and Table S11.

The presence of disproportionation products $\text{D}_{8,n}$ and $\text{D}_{9,n}$ indicate that both the primary photolysis products of Irgacure 819 (i.e., **8** and **9**) initiate polymerization. The presence of disproportionation products congruent with products involving fragment **10** evidence that secondary fragmentation of adduct **9** occurs. The spectrum in Figure 12 is less complex than the one obtained for the Irgacure/MA system. Furthermore, like the AIBN system *no* quantitative amount of monomer-initiated species are found, which is surprising as no effect on transfer to monomer rates are expected with a change in initiator type. Such an observation may simply be a result of limiting the overall chain length to the ESI mass range and hence examining the polymerization kinetics of only the oligomers in these particular cases. As expected, no polymer peaks congruent to products DMI-I_D and DMI-II_D are observed.

The Comparison of Photolysis Fragment Reactivities.

Reiterating that it is the aim of the present study to provide a “map” of initiator reactivity in photopolymerizations, it goes without saying that while the assignment of individual product spectrum yield useful information on each specific PI/monomer system under investigation, a complete picture is only drawn when all data are compiled. By collating all experimental data for the various PIs toward different monomers (including the previously studied MMA/PI systems),²² two key points of information can be assessed: First, the reactivity of the individual fragments (with respect to initiation and termination behavior) can be analyzed. Second, the reactivity of a specific fragment toward the various monomers (and therefore monomer class) may be compared. A summary of the photolysis product data is given in Table 2.

On the basis of the polymer product spectra produced under the PLP conditions examined, the reactivity of all fragment/monomer combinations under investigation have been categorized with respect to the fragment's ability to initiate and/or terminate chain propagation. These abilities are given by the symbols (listed in Scheme 5) whereby the area within the symbol given to either “i” or “t” refers to relative reactivity of the fragments. i.e. a large “i” area stands for higher propensity to initiate polymerization, while a larger “t” area indicates that the fragment is more prone to terminate chain-growth. This information is made clearer by the dominant mechanism of the fragment stressed by the size of the font of the individual letters “i” and “t”. Only two different symbols (more likely to initiate/terminate and almost exclusively initiating/terminating) are used as information as to the exact ratios depend on the relative amounts of disproportionation and combination products found in the ESI-MS spectrum which may be influenced by suppression effects as a result of end group chemistries. Fragment/monomer combinations for which the fragment is found to

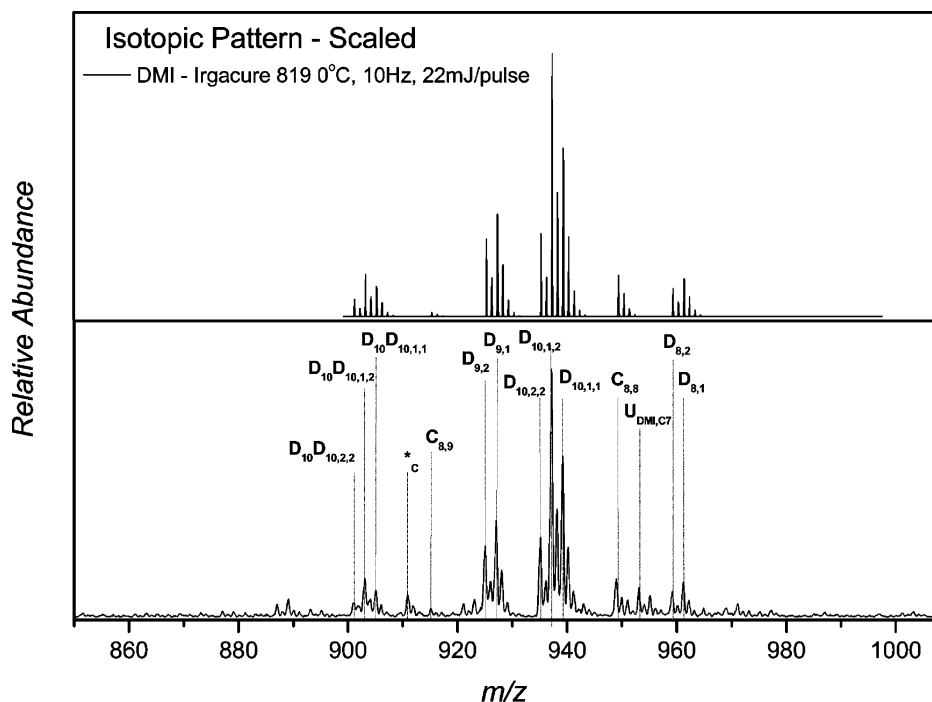


Figure 12. ESI-MS spectrum of polymeric material obtained from the Irgacure 819 initiated ($c_{\text{Irg819,0}} = 5 \times 10^{-3} \text{ mol L}^{-1}$) PLP of DMI_{bulk} (lower part). The reaction conditions are given within the figure. The theoretical isotopic pattern distribution scaled to the experimental result is given in the upper part of the figure. Theoretical product mass to charge ratios are indicated by the dotted lines.

Table 2. Reactivity of Photoinitiator Derived Fragments toward Various Monomers with Respect to Their Effectiveness to Initiate and/or Terminate Polymerization

Photolysis Fragment	MA	reactivity towards		DMI
		MMA	nBMA	
1				
2				
3 $\text{H}_3\text{C} \cdot$	x			
5				
6				
7 $\text{CH}_3\text{CH}_2 \cdot$	x	x	x	x
8				
9				
10				
11				

Scheme 5. Symbol Definitions Used in Table 2

- The fragment is found to initiate and to terminate polymerization. No clear conclusion can be drawn whether it is more prone to either reaction.
- The fragment is found to initiate and to terminate polymerization. The fragment is more effective in initiation than in termination of chain-growth.
- The fragment is found to initiate and to terminate polymerization. The fragment is more effective in termination than in initiation of chain-growth.
- The fragment is found to almost exclusively initiate the reaction.
- The fragment is found to almost exclusively terminate the reaction.
- The fragment is found to initiate the reaction. Whether it also terminates chain-growth remains unclear.
- x** The fragment could not be identified as a polymer endgroup in the product spectrum.

no background color differentiation. Such inconclusiveness may either arise from ambiguous polymer spectra, or, e.g., in the case of AIBN, from the symmetric nature of the fragments as ratios can only be assessed when two fragments are directly compared. Inability to assign products congruent with a product containing that particular fragment is indicated by an "x". It should be noted that fragment 7 (ethyl radical) was incorporated in the table as it is a potential product of a secondary cleavage reaction of fragment 6, however, it was not identified in any of our mass spectra. Further details are given in our earlier study.²²

With the exception of the DMPA photolysis fragments 1 and 2, all fragments show an equivalent behavior toward all three monomers. This observation may not only be valid for the specific monomers examined but also for the entire monomer families of which the investigated monomer are representative. Such an assumption is reasonable on the basis that no significant change in electronic factors are expected with ester side chain. Nevertheless, shielding effects might play a role but are

clearly initiate and terminate the reaction but that could not be clearly assigned with respect to their reactivity, have been labeled with a symbol where both letters have equal size and

considered to be a minor effect. A clear change in reactivity is observed for DMPA when it is examined in the DMI/DMPA system. The acetal fragment (in the MA and MMA systems at least) was found to be a better terminating species in comparison to the benzoyl fragment which was found to be highly effective in initiating polymerization. This difference in reactivity may be explained by the higher stability of the acetal fragment where the radical center is delocalized through the benzyl ring, hence increasing the lifetime of the fragment. The fact that the benzoyl fragment is clearly found to act more predominantly as a terminating species in the DMI/DMPA photopolymerization may be explained by the longer time period between propagation steps (i.e., low propagation rate coefficient). While the acetal fragment (**1**) is stable enough to persist until chain-addition takes place and is hence found as an initiating end group, the benzoyl fragment is too reactive and thus potentially terminates primary chains that have been initiated by the previous laser pulse. The same reasoning may explain why the alcohol fragment (**5**) in benzoin photocleavage does not seem to initiate acrylate and methacrylate polymerization well, but is found to initiate itaconate polymerization more efficiently, even if not over effectively. It is noteworthy to add that the acetal fragment, despite its changed propensity to initiate polymerization, still undergoes secondary cleavage to form methyl radicals, which act (exclusively) as terminating species in all systems. It may hence be concluded that DMPA is generally a much less effective initiator for DMI polymerization than for MA or MMA as lower benzoyl fragment efficiency is observed. The assignment for fragment **2**/DMI in Table 2 is based on this assumption.

The notion that the stability of the various photolysis fragments has a large influence on the initiation effectiveness of the individual fragments is suggested by the very different behavior observed for fragment **8** when compared to the benzoyl fragment **2**. The addition of the methyl groups in ortho- and para-positions to the carbonyl group appears to increase the lifetime of the radical fragment⁵³ transforming the reactivity of the species from primarily initiating to primarily terminating. This change is not inverted in the DMI photopolymerization, however, a direct comparison of fragments **8** and **2** is required because the unchanged situation for fragment **8** may only result from an overwhelmingly high initiation effectiveness of fragment **9**.^{47,48} Ideally, a photoinitiator which underwent photolysis to yield fragments **2** and **8** (presently unavailable) is required to settle conjecture over this issue.

The monomer/Irgacure 819 systems examined result in highly complex product spectra with unique features that arise from the formation of multiple generations of radicals allowing for insertion of several initiator fragments into a single chain. It is an intriguing concept that macromolecules containing fragment **9** can form block copolymers upon reinitiation under UV exposure. Investigations into the exploration of the unique behavior of Irgacure 819 are currently underway in our laboratories.

Acknowledgment. C.B.-K. is grateful for financial support from the Australian Research Council (ARC) in the form of a Discovery Grant. C.B.-K. also acknowledges receipt of an Australian Professorial Fellowship (ARC). Z.S. acknowledges financial support from the Faculty of Engineering at the University of New South Wales. S.P.S.K. acknowledges the receipt of an Australian Post Graduate Award. T.P.D. acknowledges the receipt of a Federation Fellowship (ARC). We would also like to thank Mr. Istvan Jacenyik and Dr. Leonie Barner for their excellent management of CAMD. In addition, we thank

Ciba Specialty Chemicals (Basel) for the provision of Irgacure 819 and their interest in this study.

Supporting Information Available: Figures, tables, and schemes giving experimental details. This material is available free of charge via the Internet at <http://pubs.acs.org>.

References and Notes

- (1) Gruber, H. F. *Prog. Polym. Sci.* **1992**, *17*, 953–1044.
- (2) Buback, M.; Feldermann, A.; Barner-Kowollik, C.; Lacik, I. *Macromolecules* **2001**, *34*, 5439–5448.
- (3) Buback, M.; Egorov, M.; Feldermann, A. *Macromolecules* **2004**, *37*, 1768–1776.
- (4) Szablan, Z.; Stenzel, M. H.; Davis, T. P.; Barner, L.; Barner-Kowollik, C. *Macromolecules* **2005**, *38*, 5944–5954.
- (5) Lissi, E. A.; Garrido, J. J. *Polym. Sci., Polym. Lett. Ed.* **1984**, *22*, 391–393.
- (6) Nielen, M. W. F. *Mass Spec. Rev.* **1999**, *18*, 309–344.
- (7) Raeder, H. J.; Schrepp, W. *Acta Polym.* **1998**, *49*, 272–293.
- (8) Tanaka, K. *Angew. Chem., Int. Ed.* **2003**, *42*, 3861–3870.
- (9) Saf, R.; Mirtl, C.; Hummel, K. *Acta Polym.* **1997**, *48*, 513–526.
- (10) Lovestead, T. M.; Hart-Smith, G.; Davis, T. P.; Stenzel, M. H.; Barner-Kowollik, C. *Macromolecules* **2007**, *40*, 4142–4153.
- (11) Hanton, S. D. *Chem. Rev.* **2001**, *101*, 527–569.
- (12) Montaudo, G. *Trends Polym. Sci.* **1996**, *4*, 81–86.
- (13) Scrivens, H.; Jackson, A. T. *Int. J. Mass Spectrom.* **2000**, *200*, 261–276.
- (14) Barner-Kowollik, C.; Davis, T. P.; Stenzel, M. H. *Polymer* **2004**, *45*, 7791–7805.
- (15) McEwen, C. N.; Simonsick, W. J., Jr.; Larsen, B. S.; Ute, K.; Hatada, K. *J. Am. Soc. Mass Spectrom.* **1995**, *6*, 906–911.
- (16) Vana, P.; Albertin, L.; Davis, T. P.; Barner-Kowollik, C. *J. Polym. Sci., Polym. Chem.* **2002**, *40*, 4032–4037.
- (17) Feldermann, A.; Ah Toy, A.; Davis, T. P.; Stenzel, M. H.; Barner-Kowollik, C. *Polymer* **2005**, *46*, 8448–8457.
- (18) Ah Toy, A.; Vana, P.; Davis, T. P.; Barner-Kowollik, C. *Macromolecules* **2004**, *37*, 744–751.
- (19) Vana, P.; Davis, T. P.; Barner-Kowollik, C. *Aust. J. Chem.* **2002**, *55*, 315–318.
- (20) Buback, M.; Frauendorf, H.; Vana, P. *J. Polym. Sci., Polym. Chem.* **2004**, *42*, 4266–4275.
- (21) Buback, M.; Günzler, F.; Russell, G. T.; Vana, P. Presented at the 29th Australasian Polymer Symposium, Poster Presentation; Hobart, Tasmania 2007; full article in preparation.
- (22) Szablan, Z.; Lovestead, T. M.; Davis, T. P.; Stenzel, M. H.; Barner-Kowollik, C. *Macromolecules* **2007**, *40*, 26–39.
- (23) Beuermann, S.; Buback, M.; Davis, T. P.; Gilbert, R. G.; Hutchinson, R. A.; Olaj, O. F.; Russell, G. T.; Schweer, F.; Van, Herk, A. M. *Macromol. Chem. Phys.* **1997**, *198*, 1545–1560.
- (24) Buback, M.; Kurz, C. H.; Schmaltz, C. *Macromol. Chem. Phys.* **1998**, *199*, 1721–1727.
- (25) Yee, L. H.; Coote, M. L.; Chaplin, R. P.; Davis, T. P. *J. Polym. Sci., Polym. Chem.* **2000**, *38*, 2192–2200.
- (26) Manders, B. Ph.D. Thesis, Eindhoven, **1997**; ISBN 90-386-0778-4.
- (27) Buback, M.; Kowollik, C. *Macromolecules* **1999**, *32*, 1445–1452.
- (28) Scott, G. E.; Sanogles, E. J. *Macromol. Sci. Chem.* **1974**, *753*–773.
- (29) Plessis, C.; Arzamendi, G.; Alberdi, J. M.; van Herk, A. M.; Leiza, J. R.; Asua, J. M. *Macromol. Rapid Commun.* **2003**, *24*, 173–177.
- (30) Willemse, R. X. E.; van Herk, A. M.; Panchenko, E.; Junkers, T.; Buback, M. *Macromolecules* **2005**, *38*, 5098–5103.
- (31) Junkers, T. Ph.D. Thesis, Göttingen 2006; ISBN 3-933893-51-8.
- (32) Coote, M. L.; Zammitt, M. D.; Davis, T. P. *Trends Polym. Sci.* **1996**, *4*, 189–196.
- (33) Olaj, O. F.; Bitai, I.; Hinkelmann, F. *Makromol. Chem.* **1987**, *188*, 1689–1702.
- (34) Asua, J. M.; Beuermann, S.; Buback, M.; Castignolles, P.; Charleux, B.; Gilbert, R. G.; Hutchinson, R. A.; Leiza, J. R.; Nikitin, A. N.; Vairon, J. P.; van Herk, A. M. *Macromol. Chem. Phys.* **2004**, *205*, 2151–2160.
- (35) Vana, P.; Yee, L. H.; Barner-Kowollik, C.; Heuts, J. P. A.; Davis, T. P. *Macromolecules* **2002**, *35*, 1651–1657.
- (36) Velickovic, J.; Vasovic, S. *Makromol. Chem.* **1972**, *153*, 207–218.
- (37) Fouassier, J. P.; Merlin, A. J. *Photochem.* **1980**, *12*, 17–23.
- (38) Luís Faria, J.; Steenken, S. *J. Chem. Soc., Perkin Trans.* **1997**, *2*, 1153–1159.
- (39) Heine, H. G. *Tetrahedron Lett.* **1972**, *47*, 4755–4758.
- (40) Davis, T. P.; Matyjaszewski, K. *Handbook of Radical Polymerization*; Wiley-Interscience: New York 2002.
- (41) *Polymer Handbook*, 3rd ed.; Busfield, W. K., Brandrup, J., Immergut, E. H., Eds.; Wiley-Interscience: New York 1989, p II/2–II/4.

- (42) Zammit, M. D.; Davis, T. P.; Rees, M. T. L.; Russell, G. T. *Macromolecules* **1998**, *31*, 1763–1772.
- (43) Strazielle, C.; Benoit, H.; Vogl, O. *Eur. Polym. J.* **1978**, *14*, 331–334.
- (44) Hutchinson, R. A.; Paquet, D. A.; McMin, J. H.; Beuermann, S.; Fuller, R. E.; Jackson, C. *DEHEMA Monogr.* **1995**, *131*, 467–492.
- (45) Odian, G. *Principles of Polymerization*, 4th Ed.; Wiley-Interscience: New York, 2004; p 237.
- (46) Ciba Specialty Chemicals Website; <http://www.cibasc.com/irgacure-819-dw.htm>.
- (47) Sumiyoshi, T.; Schnabel, W. *Makromol. Chem.* **1985**, *186*, 1811–1823.
- (48) Baxter, J. E.; Davidson, S. *Makromol. Chem.* **1988**, *189*, 2769–2780.
- (49) Hirano, T.; Takeyoshi, R.; Seno, M.; Sato, T. *J. Polym. Sci., Polym. Chem.* **2002**, *40*, 2415–2426.
- (50) Hirano, T.; Higashi, K.; Seno, M.; Sato, T. *J. Polym. Sci., Polym. Chem.* **2004**, *42*, 4895–4905.
- (51) Szablan, Z.; Ah Toy, A.; Terrenoire, A.; Davis, T. P.; Stenzel, M. H.; Müller, A. H. E.; Barner-Kowollik, C. *J. Polym. Sci., Polym. Chem.* **2006**, *44*, 3692–3710.
- (52) Buback, M.; Kling, M.; Schmatz, S.; Schroeder, J. *Phys. Chem. Chem. Phys.* **2004**, *6*, 5441–5455.
- (53) Benaglia, M.; Rizzardo, E.; Alberti, A.; Guerra, M. *Macromolecules* **2005**, *38*, 3129–3140.

MA070626A